Title: Optimized CART Cell Therapy for Metastatic Aggressive Thyroid Cancer

Authors: Justyna J. Gleba[1*], Elizabeth L. Siegler[2,3*], Claudia Manriquez-Roman[2,3*], Truc N. Huynh[2,3], Long K. Mai[2,3], James L. Miller[1], Erin E. Miller[1], Matthew L. Pawlush[1], Aylin Alasonyalilar Demirer[1], Brooke L. Kimball[2,3], Erin E. Tapper[2,3], R. Leo Sakemura[2,3], Carli M. Stewart[2,4,5], Ismail Can[2,3], Olivia L. Sirpilla[2,4,5], Jennifer M. Feigin[2,4,6], Kun Yun[2,4,7], Omar L. Gutierrez Ruiz[2,3], Hong Xia[2,3], Mehrdad Hefazi Torghabeh[2,3], Kendall J. Schick[2,3], Ekene J. Ogbodo[2,3], Gloria Olivier, PhD[8], Yushi Qiu[1], Han W. Tun[9], Robert C. Smallridge[10], Abba Zubair[11], John A. Copland[1], and Saad S. Kenderian[2,3,4,7,12]

Affiliations:

[1] Cancer Biology Department, Mayo Clinic, Jacksonville, FL

[2] T Cell Engineering, Mayo Clinic, Rochester, MN

[3] Division of Hematology, Mayo Clinic, Rochester, MN

[4] Mayo Clinic Graduate School of Biomedical Sciences, Rochester, MN

[5] Department of Molecular Pharmacology and Experimental Therapeutics, Mayo Clinic, Rochester, MN

[6] Department of Biochemistry and Molecular Biology, Mayo Clinic, Rochester, MN

[7] Department of Molecular Medicine, Mayo Clinic, Rochester, MN

[8] Department of Business Development, Mayo Clinic, Rochester, MN

[9] Hematology/Oncology Division, Department of Medicine, Mayo Clinic, Jacksonville, FL

[10] Endocrine Division, Internal Medicine Department, Mayo Clinic, Jacksonville, FL

[11] Department of Laboratory Medicine and Pathology, Mayo Clinic, Jacksonville FL

[12] Department of Immunology, Mayo Clinic, Rochester, MN

* Contributed equally

Corresponding authors: Saad S. Kenderian, Mayo Clinic Rochester, 200 First Street S.W., Rochester, MN Kenderian.saad@mayo.edu, *or* John A. Copland, Mayo Clinic Florida, copland.john@mayo.edu

Running Title: TSHR-CART cell therapy in thyroid cancers

Acknowledgements: This study was partly funded through Mayo Clinic Center for Regenerative Biotherapeutics (SSK and JAC), Mayo Clinic Comprehensive Cancer Center (SSK), National Institutes of Health R37CA266344-01 (SSK), and Department of Defense grant CA201127 (SSK)

Competing Interests: SSK is an inventor on patents in the field of CAR immunotherapy that are licensed to Novartis (through an agreement between Mayo Clinic, University of Pennsylvania, and Novartis), and MustangBio (through Mayo Clinic). RLS and SSK are inventors on patents in the field of CAR immunotherapy that are licensed to Humanigen (through Mayo Clinic). MH and SSK are inventors on patents in the field of CAR immunotherapy that are licensed to Mettaforge (through Mayo Clinic). SSK receives research funding from Kite, Gilead, Juno, BMS, Novartis, Humanigen, MorphoSys, Tolero, Sunesis/Viracta, LifEngine Animal Health Laboratories Inc, and Lentigen. SSK has participated in advisory board meetings with Kite/Gilead, Humanigen, Juno/BMS, Capstan Bio, Luminary, and Novartis. SSK has served on the data safety and monitoring board with Humanigen and Carisma. SSK has served as a consultant for Torque, Calibr, Novartis, Capstan Bio, Kite, Carisma, and Humanigen.

ABSTRACT

Most thyroid cancer deaths are attributed to a subset of poorly differentiated, metastatic tumors. To improve treatment options for these aggressive thyroid cancers, we developed a novel thyroid-stimulating hormone receptor (TSHR)-targeted chimeric antigen receptor T (CART) cell therapy, which demonstrated antigen-specific activation and antitumor efficacy against TSHR-overexpressing cell lines *in vitro* and *in vivo*. However, de-differentiated thyroid cancers downregulate TSHR. We therefore developed a potent treatment strategy by combining our novel TSHR-CART cells with mitogen-activated protein kinase (MAPK) inhibitors, which redifferentiate thyroid tumors and upregulate TSHR expression. In patient-derived anaplastic thyroid cancer xenografts, combination therapy of TSHR-CART cells and MAPK inhibitors led to increased TSHR expression on the tumor tissue and significantly enhanced antitumor efficacy and prolonged survival compared to TSHR-CART monotherapy.

STATEMENT OF SIGNIFICANCE

Poor target selection and antigen escape limit CART cell efficacy in solid tumors. We developed TSHR-CART cells to treat differentiated thyroid cancers but observed TSHR downregulation in dedifferentiated thyroid cancers. We found that MAPK inhibitors restored TSHR expression and sensitized these cancers to TSHR-CART cell therapy.

INTRODUCTION

Thyroid cancer is the most common endocrine cancer, and its incidence is rising in the US and globally.(1,2) Thyroid cancer is projected to become the fourth leading type of cancer across the world, and the causes appear to be complex and multifactorial, including dietary changes and environmental exposures. Patients with thyroid cancer have widely different clinical outcomes depending on the pathological subtype and mutation profile. Metastatic differentiated thyroid cancer (DTC), poorly differentiated thyroid cancer (PDTC), and anaplastic thyroid cancer (ATC) account for a majority of thyroid cancer-related deaths, even though these subtypes only represent 2-3% of all thyroid cancer diagnoses.(1,3,4) Hurthle cell carcinoma (HCC, now termed oncocytic thyroid cancer(5)) is a subtype of DTC known to be aggressive, highly metastatic, and have lower rates of overall survival than follicular thyroid cancers. HCC is often resistant to radioiodine therapy and has no current FDA-approved treatment options.(6,7) PDTC and ATC are aggressive and often refractory to radioiodine therapy and other standard therapies.(8,9) SEER database analysis through 2015 reported a median overall survival of 4 months in patients with ATC, with disease-specific mortality of over 98%. A more recent analysis reported a median overall survival of 15.7 months in patients with ATC receiving newer targeted therapies.(10) Despite these advancements in treatment options, PDTC and ATC remain incredibly lethal.

Chimeric antigen receptor (CAR) T cell therapy has emerged as a potentially curative therapy in a subset of patients with hematological malignancies and has been FDA-approved for several B cell malignancies as well as for multiple myeloma.(11-15) With the advent of adoptively transferred engineered cellular therapies, there is a compelling rationale to apply CART cell therapy to treatment-resistant solid tumors. To date, the efficacy of CART cell therapy in solid tumors has been modest at best.(16-21) Due to a lack of tumor-specific targets for CART cell therapy in solid tumors, identifying an antigen that is both uniquely and universally expressed on cancer cells is critical for development of antigen-specific immunotherapy to avoid on-target off-tumor toxicities.(20,22,23)

Thyroid-stimulating hormone receptor (TSHR) is a surface glycoprotein receptor and a major regulator of thyroid function and metabolism. The TSHR mediates the activating mechanism of TSH to the thyroid gland, resulting in the growth and proliferation of thyrocytes as well as thyroid hormone production, including thyroxine (T4) and triiodothyronine (T3).(24) TSHR is predominantly expressed on the basolateral membrane of normal thyroid follicular cells.(25) TSHR expression is largely limited to the thyroid gland, with moderate/low levels of expression in the thymus and testes. TSHR is abundantly expressed on thyroid tumor cells.(25,26) Given its unique expression, TSHR is recognized as a compelling target for advanced thyroid cancer diagnostics and therapy

after thyroidectomy. Overall, there is limited risk of off-tumor adverse effects of targeting TSHR. TSHR has been targeted using biologics including monoclonal antibodies for the treatment of Graves' disease and thyroid cancer.(27) In this study, we generated CART cells targeting TSHR (TSHR-CART) and showed potent, antigen-specific antitumor efficacy against TSHR-expressing cell lines *in vitro* and *in vivo,* as well as in patient-derived xenograft (PDX) mouse models of ATC.

Further, we identified mitogen-activated protein kinase (MAPK) inhibition as a strategy to upregulate TSHR in dedifferentiated thyroid cancers and increase the therapeutic index of TSHR-CART cell therapy. Downregulation of TSHR expression in dedifferentiated thyroid cancer is a potential mechanism of resistance to TSHR-CART cell therapy. MAPK inhibition is an FDA-approved treatment against thyroid cancer and is documented to upregulate TSHR expression in patients with advanced metastatic thyroid cancer.(28,29) Clinical trials for metastatic thyroid cancers have demonstrated that MAPK inhibition induces re-expression of genes necessary for iodine uptake and retention, including TSHR and sodium iodide symporter (NIS).(30,31) Additionally, many thyroid cancers have gene mutations involving the constitutive activation of BRAF, which stimulates MAPK signaling.(32-34) Therefore, when BRAF activation is switched off genetically, or its downstream signaling is inhibited with MEK or BRAF inhibitors, tumors re-express TSHR and NIS and reaccumulate iodine. This strategy has been employed in the clinic to enhance the response to radioactive iodine therapy.(29)

We therefore sought to address antigen escape in ATC by testing the combination of MEK/BRAF small molecule inhibitors with TSHR-CART cell therapy. We found that MEK/BRAF inhibition led to restoration of TSHR expression on thyroid cancer cells and enhancement of CART cell expansion and antitumor activity *in vivo*. We further improved CART antitumor efficacy by changing the duration of MEK/BRAF inhibitor administration. This strategy is highly translatable to a patient population with extremely limited treatment options to date.

RESULTS

TSHR as a target for CART cell therapy

To validate TSHR as a target candidate for CART cell therapy in thyroid cancer, we verified its expression on thyroid tissue and lack of expression on other normal tissues by immunohistochemistry (IHC) analysis of specimens from the Mayo Clinic Thyroid Cancer Biobank and on publicly available Human Protein Atlas data.(35) IHC analysis showed that, while TSHR expression was high in normal thyroid tissue as well as multiple thyroid cancer histotypes, ATC samples demonstrated attenuated TSHR expression (**Figure 1A, B**). Having validated

TSHR as a potential antigen to target with CART cell therapy, we designed and generated TSHR-CART cells using a single chain variable fragment isolated from the TSHR autoantibody clone K1-70 and cloned into a third-generation lentiviral CAR construct containing 4-1BB and CD3ζ (**Supplementary Figure 1A**). Healthy donor T cells transduced with CAR-encoded lentiviral particles (**Supplementary Figure 1B**) demonstrated high CAR expression as assessed by flow cytometry (**Figure 1C**).

TSHR-CART cells exhibit potent and specific antitumor activity against TSHR-expressing tumor cells *in vitro*

We next examined the antigen-specific activation of TSHR-CART cells *in vitro* and *in vivo*. TSHR-CART cells or control untransduced T cells (UTD) were incubated with the follicular thyroid cancer cell line, FTC133, which was transduced to overexpress TSHR. Compared to UTD, TSHR-CART cells demonstrated profound antigen-specific effector functions against $TSHR^{+}$ target cells *in vitro*, including cytotoxicity against target cells (**Figure 1D**) as well as TSHR-CART proliferation (**Figure 1E**), degranulation (**Figure 1F**), and cytokine production (**Figure 1G**). To confirm antigen specificity, we cocultured TSHR-CART cells with the $TSHR^{-}$ cell line, Nalm6, and did not observe significant cytotoxicity (**Supplementary Figure 1C**) or proliferation (**Supplementary Figure 1D**).

TSHR-CART cells show durable antitumor activity in xenograft models of HCC

We then assessed TSHR-CART cell activity in a xenograft model of HCC. We first measured TSHR expression via IHC on biopsies obtained from patients with normal thyroid tissue, primary HCC with minimal or extensive invasion, locally recurrent HCC, and metastatic HCC. Strong TSHR expression was maintained in recurrent and metastatic lesions as well as primary tumors (**Figure 2A-B**). Next, non-obese diabetic severe combined immunodeficiency $IL2r\gamma^{-}/^{-}$ (NSG) mice were subcutaneously engrafted with 10×10^{6} HCC cell line XTC.UC1, which has high endogenous TSHR expression (**Supplementary Figure 1E**) and treated with 10×10^{6} UTD or TSHR-CART cells when tumors reached ~$100mm^{3}$. Serial caliper measurements revealed significant antitumor efficacy of TSHR-CART cells compared to UTD control (**Figure 2C**). At Day 50 post-engraftment, all UTD-treated mice had reached humane endpoints, while all TSHR-CART-treated mice were in remission or had small tumors (**Figure 2D**). Three TSHR-CART-treated mice in remission were then rechallenged on Day 51 with XTC.UC1 in the opposite flank and were followed for tumor growth along with a new group of untreated XTC.UC1-bearing

mice as controls. Again, TSHR-CART cells displayed potent antitumor activity; both original and rechallenged tumors were significantly suppressed compared to untreated controls (**Figure 2E**). Peripheral blood sampling at 21 days post-tumor rechallenge revealed significantly higher numbers of human $CD3^+$ T cells in TSHR-CART-treated mice compared to controls (**Figure 2F**). These data demonstrated that TSHR-CART cells exerted durable tumor control in an aggressive disease setting with no current standard of care.

TSHR-CART cells demonstrate strong antitumor effects in PDX models of PDTC

Next, we evaluated the antitumor activity of TSHR-CART cells in a PDX model in NSG mice. Here, we utilized aggressive, BRAF-mutant, patient-derived PDTC cells, THJ-529T, which were transduced to overexpress TSHR. Mice were subcutaneously injected with 2.5 x 10^6 THJ-529T cells, and engraftment was confirmed by caliper measurement of tumor masses. When tumors reached ~100mm^3, mice were randomized to treatment with 5 x 10^6 UTD, 5 x 10^6 TSHR-CART cells, or 10 x 10^6 TSHR-CART cells (**Figure 3A**). Treatment with TSHR-CART cells led to significant and dose-dependent tumor control (**Figure 3B-E, Supplemental Figure 2A-C**), improved survival outcomes (**Figure 3F, Supplemental Figure 2D**), increased tumor-infiltrated human T cells (**Figure 3G-H**), and increased human T cell proliferation in the peripheral blood (**Supplemental Figure 2E**).

TSHR is downregulated in ATC but is restored with MEK inhibition

ATC cells have been associated with de-differentiation and downregulation of TSHR expression, and we showed that ATC significantly downregulated TSHR expression compared to normal thyroid tissues or more differentiated thyroid cancers (**Figure 1A, B**). This observed downregulation raises concerns for antigen escape and subsequent resistance to TSHR-CART cell therapy. We first verified that the MEK inhibitor, trametinib, restored TSHR expression and reduced tumor growth in an ATC PDX model. In this model, 5mm^3 Th-560 ATC PDX tissue was surgically implanted into the right lateral flank of NSG mice and grown to approximately 100mm^3. Mice then received daily treatment with either vehicle control or trametinib at the indicated doses until the experimental endpoint (**Figure 4A**). The administration of trametinib resulted in significant dose-dependent tumor reduction (**Figure 4B**) as well as TSHR re-expression which inversely correlated with pERK expression (**Figure 4C**) after one week of daily trametinib treatment compared to placebo treatment. Because many ATC tumors are BRAF-mutant, we performed a similar experiment in which mice received either vehicle control or the dual MEK/BRAF inhibitor R05126766 at the indicated doses. Treatment with R05126766 resulted in a significant dose-dependent tumor reduction (**Figure 4D**), and pERK expression inversely correlated with TSHR expression (**Figure 4E**) after

one week of daily R05126766 treatment compared to placebo treatment. Similarly, treatment with combination trametinib (MEK inhibitor) and dabrafenib (BRAF inhibitor) resulted in significantly increased TSHR expression in ATC PDX models (**Supplementary Figure 3A-B**). Collectively, these data support the therapeutic strategy of MEK and BRAF inhibitor treatment to re-express TSHR and thereby reduce ATC resistance to TSHR-CART cell therapy.

MEK and BRAF inhibition does not negatively impact TSHR-CART cell activity

Therefore, we aimed to evaluate MEK and BRAF inhibition as a strategy to upregulate TSHR expression on thyroid cancer cells and increase the therapeutic index of TSHR-CART cell therapy. Prior to developing MEK and BRAF inhibition as a strategy to redifferentiate cancer cells in the context of TSHR-CART cell therapy, we aimed to rule out any detrimental effects of MEK or BRAF inhibition on CART cell activity, given that T cells are shown to utilize MAPK signaling. TSHR-CART proliferation, degranulation, and intracellular cytokine production were not affected by the addition of MEK or BRAF inhibitors compared to media control (**Figure 5A-C**).

Continuous MEK and BRAF inhibition yields superior TSHR-CART cell activity

Having shown that the addition of MEK and/or BRAF inhibitors was not detrimental to CART function, we next studied the kinetics of TSHR expression after MEK/BRAF inhibition to determine the longevity of TSHR re-expression after treatment with MEK/BRAF inhibitors. Mice were implanted with 5mm^3 Th-560 ATC PDX tumors. When tumors reached ~100mm^3, mice were treated daily with either vehicle control or with 1.5 mg/kg dual MEK/BRAF inhibitor R05126766 plus 1 mg/kg dabrafenib. TSHR protein expression was assessed by IHC and was found to be significantly elevated after 7 days of MEK/BRAF inhibitor treatment compared to vehicle control. However, TSHR expression was subsequently lost within two days after stopping MEK/BRAF inhibitor treatment (**Figure 6A**).

Given these results, we compared different dosing regimens of MEK/BRAF inhibitors in combination with TSHR-CART cell therapy in ATC PDX models to determine if sequential or concurrent MAPK inhibitor administration yielded superior CART antitumor activity. Mice were implanted with 5mm^3 Th-560 ATC PDX tumors. When tumors reached ~100mm^3, mice were treated daily with vehicle control, 0.25 mg/kg trametinib (continuously administered or stopped after 7 days), or 0.25 mg/kg trametinib plus 2 mg/kg dabrafenib (continuously administered or stopped after 7 days). Mice treated with vehicle control were engrafted with tumor one week

later than mice treated with MEK/BRAF inhibitors to ensure equal tumor sizes across all groups when UTD or TSHR-CART cells were administered. Mice were then given 10 x 10^6 UTD or TSHR-CART cells via tail vein injection. Tumor volume, body weight, and body condition were inspected to monitor disease progression and to assess for endpoint criteria (**Figure 6B**). Mice treated with continuous MEK inhibitors or continuous MEK and BRAF inhibitors in combination with TSHR-CART cells (CART + MEK and CART + MEK + BRAF, respectively) showed superior antitumor efficacy (**Figure 6C-D, Supplementary Figure 4A-F, Supplementary Figure 5A-F**). These findings indicate that continuous MAPK inhibition of de-differentiated thyroid cancers most effectively upregulates TSHR expression and enhances the antitumor activity of TSHR-CART cell therapy.

DISCUSSION

Here, we describe the development and evaluation of a highly translational CART cell therapy for the treatment of poorly differentiated, anaplastic, and metastatic thyroid cancers. TSHR is a rational target for CART cell therapy, given that it is widely expressed in thyroid cancers and rarely expressed outside the thyroid. We subsequently generated and tested TSHR-CART cells, which demonstrated antigen-specific activity against TSHR-expressing target cells *in vitro* and *in vivo*. HCC represents ~4% of thyroid cancers and is typically radioiodine-resistant for metastatic disease, retains TSHR expression, and currently has no FDA-approved therapy.(7,36) Our data demonstrate that TSHR-CART cell therapy resulted in durable remissions *in vivo* and may represent a treatment option for this subset of patients.

De-differentiated and anaplastic thyroid cancers can exhibit significant downregulation of thyroid developmental genes, including TSHR.(37,38) This phenomenon poses a formidable hurdle to effective TSHR-CART treatment. Increasing evidence indicates that TSHR downregulation and de-differentiation is mediated by MAPK signaling.(28,29,34,39,40) The majority of thyroid cancers have activating oncogenic gene mutations involving PI3K, RET, RAS, and BRAF.(32) Constitutive activation of these proteins stimulates MAPK signaling, inhibiting the expression of thyroid hormone biosynthesis genes.(33,34) Therefore, when BRAF activation is switched off genetically or its downstream signaling is inhibited with MEK or BRAF inhibitors, tumors re-express TSHR and reaccumulate iodine. Such a strategy has been employed in the clinic to enhance the response to radioactive iodine therapy.(30) Recent findings from patients with thyroid cancer who have been treated with MEK inhibitors indicate a dramatic upregulation of TSHR within both primary and secondary thyroid cancer tumors.(30,41) Additionally, MEK inhibitors, alone or in combination with BRAF inhibitors, demonstrate significant antitumor

activity in metastatic thyroid cancer and are FDA-approved for ATC.(42) We therefore tested the combination of TSHR-CART cell therapy plus MEK/BRAF inhibition to upregulate TSHR expression in the tumor and enhance CART efficacy, demonstrating restoration of TSHR expression and improved CART antitumor effects in mice receiving combination therapy compared to mice receiving CART monotherapy.

Major limitations to effective CART cell therapy in solid tumor settings include appropriate target antigen selection, antigen-negative escape, and lack of T cell infiltration into the tumor site. The treatment strategy we have outlined here has strong potential to overcome these limitations, as TSHR is nearly uniquely and universally expressed in thyroid tumors, MEK/BRAF inhibition induces TSHR re-expression, and TSHR-expressing advanced thyroid tumors are commonly infiltrated by immune cells, including T cells.(9) CART cells targeted against ICAM-1(43) and GFRα4(44) have demonstrated efficacy in preclinical thyroid cancer models. Recently, TSHR-CART cell therapy displayed potent activity against human thyroid cancer models *in vivo.*(45) Furthermore, two patients with high metastatic burden and iodine-131-resistant thyroid cancer demonstrated a complete response (CR) and a near CR after TSHR-CART treatment.(46) However, these studies focused on differentiated thyroid cancers with high TSHR expression. One patient with iodine-refractory, metastatic PDTC was treated with CART cells targeting both TSHR and CD19. This patient achieved stable disease at day 30 post-CART infusion and partial response 90 days post-CART infusion. While IHC demonstrated strong TSHR expression pre-CART infusion, it is unknown if TSHR was downregulated after the start of TSHR-CART cell therapy, leading to underwhelming therapeutic response in this dedifferentiated thyroid cancer setting.(47)

We present TSHR-CART cell therapy in combination with MEK/BRAF inhibition as a sensitizing modality, representing a major step forward in the development of a treatment strategy for PDTC and ATC as well as DTCs which have become refractory to radioiodine therapy.

MATERIALS AND METHODS

Cell lines

FTC133, XTC.UC1, and THJ529T cell lines were graciously provided by Dr. Copland's lab of Mayo Clinic, Jacksonville, Florida. FTC-133 cell line is derived from a differentiated follicular thyroid carcinoma with known mutations that include *FLCN, MSH6, NF1, PTEN, TERT*, and *TP53* (https://www.cellosaurus.org/CVCL_1219). THJ-529T cell line was derived from a PDTC tumor containing *BRAF* and *TERT* mutations (https://www.cellosaurus.org/CVCL_9916).(48) XTC.UC1 is the only characterized HCC cell line and the only

known cell line to express TSHR.(49) K562 cells were obtained from ATCC (Manassas, VA, USA). All cell lines were DNA short tandem repeat (STR) validated prior to use. For indicated experiments, K562 and FTC133 cell lines were transduced with a firefly luciferase vector containing a hygromycin resistance gene (Promega, Madison, WI, USA) as well as a TSHR vector containing GFP and a puromycin resistance gene (Genecopoeia Inc., Rockville, MD, USA). These cells were then cultured in selection media containing either hygromycin (1 µg/mL) or puromycin (1 µg/mL) to obtain a pure population as previously described.(50) K562 cell lines were cultured in R10 medium made with RPMI 1640 (Gibco, Gaithersburg, MD, USA), 10% fetal bovine serum (FBS, Sigma, St. Louis, MO, USA), and 1% penicillin-streptomycin-glutamine (PSG, Gibco, Gaithersburg, MD, USA). FTC133 and XTC.UC1 cell lines were cultured in D10 medium made with DMEM (Corning Inc., Corning, NY, USA), 10% FBS (Sigma, St. Louis, MO, USA), and 1% PSG (Gibco, Gaithersburg, MD, USA).

CAR construct and CART cell production

The use of recombinant DNA in the laboratory was approved by the Mayo Clinic Institutional Biosafety Committee (IBC), IBC number HIP00000252.20. Peripheral blood mononuclear cells (PBMCs) were isolated from de-identified normal donor blood apheresis cones(51) obtained under a Mayo Clinic IRB approved protocol, using SepMate tubes (STEMCELL Technologies, Vancouver, BC, Canada) and Lymphoprep™ solution (STEMCELL Technologies, Vancouver, BC, Canada). T cells were separated with negative selection magnetic beads using EasySep™ Human T Cell Isolation Kit (STEMCELL Technologies, Vancouver, BC, Canada). Second-generation 4-1BB- costimulated TSHR CAR constructs were synthesized *de novo* (IDT, Coralville, USA) and cloned into a third-generation lentivirus under the control of the EF-1α promotor. The TSHR-targeted single chain variable fragment was derived from an autoantibody from a patient with Graves' disease, clone K1-70.(52) TSHR-CART cells were then generated through the lentiviral transduction of normal donor T cells as previously described. Briefly, lentiviral particles were generated through the transient transfection of plasmid into 293T virus-producing cells (ATCC, Manassas, VA, USA) in the presence of Lipofectamine 3000 (Invitrogen, Carlsbad, CA, USA), vesicular stomatitis virus G (VSV-G), and packaging plasmids pCMVR8.74 (Addgene, Cambridge, MA, USA). The titers and multiplicity of infection (MOI) were analyzed and calculated by flow cytometry as previously described.(50) T cells isolated from normal donors were stimulated using anti-CD3/CD28 Dynabeads (Life Technologies, Oslo, Norway) at a 3:1 beads-to-cell ratio and then transduced 24 hours after stimulation with lentivirus particles at a MOI of 3. T cells were cultured in T cell medium containing X-VIVO™ 15 media (Lonza,

Basel, Switzerland), 10% human AB serum (Corning Inc., Corning, NY, USA), and 1% PSG (Gibco, Gaithersburg, MD, USA). Magnetic bead removal and the evaluation of CAR expression on T cells by flow cytometry were performed on day 6 by staining with a goat anti-mouse F(ab')2 antibody (Invitrogen, Carlsbad, CA, USA). CART cells were harvested and cryopreserved on day 8 for future experiments. CART cells were thawed and rested in T cell medium overnight at 37°C and 5% CO_2 prior to experimental use.

Multi-parametric flow cytometry

Anti-human antibodies were purchased from Biolegend (San Diego, CA, USA), eBioscience (San Diego, CA, USA) or BD Biosciences (San Jose, CA, USA). Samples were prepared for flow cytometry as previously described.(50,53-56) In all analyses, the population of interest was gated based on forward vs side scatter characteristics, then by singlet gating, and then by live cell gating using LIVE/DEAD™ Fixable Aqua Dead Cell Stain Kit (Invitrogen, Carlsbad, CA, USA). Flow cytometry was performed on a three-laser CytoFLEX (Beckman Coulter, Chaska, MN, USA). All analyses were performed using FlowJo v10.7.1 software (Ashland, OR, USA).

Immunohistochemistry (IHC)

IHC was performed on paraffin-embedded tissue. Thyroid tissue microarray (TMA) was made from archival samples under Mayo Clinic IRB approval with sample size for each tumor at 1.5 mm. Paraffin blocks were cut into 5 μm thick sections. Slides were deparaffinized, rehydrated with decreasing concentrations of ethanol, and finally with water. Antigen retrieval was performed using Antigen Retrieval Solution (pH 6 or pH 9) (Dako, Glostrup, Denmark) for at least 15 minutes in an autoclave, and cooling for 30 minutes at room temperature. Slides were washed with 3% hydrogen peroxide (Fisher Scientific, Waltham, MA, USA) for 10 minutes to block the activity of endogenous peroxidases. Primary anti-human TSHR antibody was used for 60 minutes at room temperature at 1:500 (abcam, ab218108, Cambridge, UK). The infiltration of human T lymphocytes into the neoplastic tumors was assessed using anti-human CD3 at 1:500 (abcam, ab52959, Cambridge, UK). The primary antibody was detected using the Envision Labeled Kit (Dako, Glostrup, Denmark) according to the manufacturer's protocol. After washing, slides were counterstained with Mayer's hematoxylin (Sigma-Aldrich, St. Louis, MO, USA). Slides were dehydrated through ethanol and xylene and cover-slipped using a xylene-based mounting medium (Fisher Scientific, Waltham, MA, USA). Samples were examined under bright-field illumination at 20x objective, and digital images were obtained using Aperio AT2 (Leica, Wetzlar, Germany). Results were processed using Aperio eSlide Manager and H-Score values were estimated using the Aperio ImageScope

Software (both Aperio Technologies, Vista, CA, USA). The staining of the TMA punches was scored using an algorithm in the Imagescope Software (Aperio Technologies, Vista, CA, USA) created by a histologist based upon signal intensity (0, 1C, 2C, 3C). H score was then calculated based upon signal intensity and percentage: HZ(1C%!1)(2C%!2)(3C%!3). Cases were excluded from the study if a section could not be assigned a score due to insufficient quantity of tumor tissue present**.** Normal tissues were used as a positive and negative control.

For cell line preparation for IHC, cells were washed three times with PBS (Corning, NY, USA), scraped from the bottom of the plate using a cell lifter (Fisherbrand, Waltham, MA, USA), transferred to 50 mL polypropylene tubes and centrifuged at room temperature for 2 minutes at 500 x g. The supernatant was aspirated, and 10% neutral buffered formalin (Fisher Scientific, Waltham, MA, USA) was added for 30 minutes at room temperature. HistoGel (Thermo Scientific, Waltham, MA, USA) was heated in the microwave for 3 seconds at maximal power and converted to a liquid state. Cells were transferred to the HistoScreen Tissue Cassettes (Thermo Scientific, Waltham, MA, USA) and covered with liquid Histogel. Samples were placed at room temperature and allowed to solidify. HistoGel blocks were transferred into tissue embedding cassettes (Thomas Scientific, Swedesboro, NJ, USA), dehydrated in increasing concentrations of ethanol, xylene, and paraffin embedding. Sections were prepared as described in the immunohistochemistry section. Primary anti-human TSHR antibody was used for 60 minutes at room temperature at 1:1500 (abcam, ab218108, Cambridge, UK). Envision labeled polymer (Dako, Glostrup, Denmark) was used for 30 minutes as a secondary antibody. Slides were stained with diaminobenzidine tetrahydrochloride (DAB) chromogen (Dako, Glostrup, Denmark) for 5 minutes at room temperature and counterstained with Mayer's hematoxylin (Sigma-Aldrich, St. Louis, MO, USA). Control staining with hematoxylin and eosin (Sigma-Aldrich, St. Louis, MO, USA) was also performed. Aperio AT2 scanner (Leica, Wetzlar, Germany) was used for the digital image, at 20x objective. Images were analyzed using the Aperio ImageScope software (Aperio Technologies, Vista, CA, USA).

Immunocytochemistry (ICC)

THJ-529 cells (2 x 10^4 cells/chamber) were plated in a 4-well chamber slide (Nunc, Thermo Scientific, Waltham, MA, USA), incubated overnight. After 24 hours, media was aspirated, and cells were washed three times with PBS (Corning, NY, USA). Then, 2% paraformaldehyde was added for 20 minutes at room temperature. Again, cells were washed three times with PBS. Next, ice-cold 100% methanol (Fisher Scientific, Waltham, MA, USA) was added for 7 minutes at -20°C. Methanol was aspirated, and samples were allowed to air dry for 10 minutes.

Next, serum-free-blocking diluent (Dako, Glostrup, Denmark) was used for 30 minutes at room temperature. Primary anti-human TSHR antibody was used for 60 minutes at room temperature at 1:1500 (abcam, ab218108, Cambridge, UK). Slides were subsequently prepared as described in the immunohistochemistry section.

***In vitro* T cell function assays**

Proliferation assays were performed as previously described.(50,53-56) UTD or TSHR-CART cells were re-suspended in T cell medium at 1×10^6/mL, and 100 µL per well were seeded in 96-well plates. Each assay included T cells with media only as a negative control and T cells with PMA and ionomycin as a positive control. After five days, cells were harvested and stained with APC-H7 anti-human CD3 (BD Biosciences, Franklin Lakes, NJ, USA) and LIVE/DEAD™ Fixable Aqua.

Cytotoxicity assays were performed as previously described.(50,53-56) Luciferase$^+$ TSHR$^+$ K562 or TSHR$^+$ FTC133 cells were used as target cells. UTD or TSHR-CART cells were co-cultured with target cells at various effector: target (E:T) ratios in T cell medium. Cytotoxicity was calculated by bioluminescence imaging on the Promega GloMax Explorer (Promega Corporation, Fitchburg, WI, USA) as a measure of residual live cells at indicated time points. Samples were treated with 1µl D-luciferin (30µg/mL) per 100µl sample volume (Gold Biotechnology, St. Louis, MO, USA) prior to imaging.

Degranulation and intracellular cytokine assays were performed as previously described.(50,53-56) UTD or TSHR-CART cells were incubated with various target cells at an E:T ratio of 1:5. Antibodies against CD107a (clone H4A3) FITC (BD Pharmingen, San Diego, CA, USA, Cat# 555800), CD28 (BD Biosciences, San Diego, CA, USA, Cat# 348040), CD49d (BD Biosciences, San Diego, CA, USA, Cat# 340976) and monensin (Biolegend, San Diego, CA, USA, Cat# 420701) were added prior to the incubation. After 4 hours, cells were harvested and stained with LIVE/DEAD™ Fixable Aqua. Cells were then fixed and permeabilized (FIX & PERM Cell Fixation & Cell Permeabilization Kit, Life Technologies, Oslo, Norway) and stained for CD3 (clone UCHT1) APC (Cat# 17-0038-42, eBioscience, San Diego, CA, USA) and intracellular cytokines including IL-2 (clone 5344.111) PE-CF594 (BD Pharmingen, San Diego, CA, USA, Cat# 562384), GM-CSF (clone BVD2-21C11) BV421 (BD Pharmingen, San Diego, CA, USA, Cat# 562930), and MIP1-β (clone D21-1351) PE-Cy7 (BD Pharmingen, San Diego, CA, USA, Cat# 560687).

***In Vivo* Models**

Male and female 6-8-week-old NOD-SCID-IL2rγ^{-}/$^{-}$ (NSG) mice were obtained from Jackson Laboratories

(Jackson Laboratories, Bar Harbor, ME, USA) and maintained in an animal barrier space that is approved by the institutional Biosafety Committee for BSL2+ level experiments at the Mayo Clinic animal facility (IBC #HIP00000252.20). Mice were treated on an IACUC-approved protocol (A00001767).

In cell line xenograft models, 2.5 x 10^6 $TSHR^+$ THJ529 or 10 x 10^6 XTC.UC1 cells were suspended in a 50% Matrigel basement medium and subcutaneously injected into the rear flank of NSG mice. Serial caliper measurements were performed to confirm tumor engraftment. Mice were then randomized based on tumor burden to receive different treatments as outlined in the specific experiment. Tumor growth was monitored by serial caliper measurements (width x height x length x 0.523 = mm^3). Mice were euthanized once IACUC-approved endpoint criteria were met, and remaining tumors were collected for IHC as indicated in the specific experiment.

In ATC PDX models, NSG mice were surgically engrafted with $5mm^3$ ATC PDX tumors in their rear flank. In TSHR upregulation experiments, mice were treated with the indicated doses of MEK/BRAF inhibitors (trametinib, dabrafenib, or R05126766). Upon euthanasia, tumors were harvested for IHC. In MAPK inhibitor and TSHR-CART combination experiments, upon tumor engraftment, mice were treated with a sub-therapeutic dose of 1mg/kg trametinib and 1.5mg/kg dabrafenib as a sensitizing regimen to induce TSHR expression on ATC tumor cells. On Day 7, additional mice were surgically engrafted with $5mm^3$ ATC PDX tumors in the same manner as the first arm but were treated with placebo rather than MAPK inhibitors. When tumors reached ~$100mm^3$, all mice were randomized based on tumor burden and injected with 10 x 10^6 UTD or TSHR-CART. Disease progression was monitored through serial assessment of tumor volume with caliper measurements. Weekly tail vein bleeding after injection of CART cells was performed to assess T cell expansion. Mouse peripheral blood was lysed using BD FACS Lyse (BD Biosciences, San Diego, CA, USA) and then analyzed with flow cytometry as previously described.(50,57) Mice were euthanized at IACUC-approved endpoints.

Statistical analysis

GraphPad Prism (La Jolla, CA, USA) and Microsoft Excel (Microsoft, Redmond, WA, USA) were used to analyze raw experimental data. Statistical tests are described in figure legends.

Author Contribution

JJG, ELS, and CMR wrote, reviewed, and edited manuscript, designed and performed experiments, and

analyzed data. JJG, JLM, EEM, AAD, TNH, LKM, BLK, EET, RLS, ELS, CMS, IC, OLS, KY, JMF, OLGR, HX, MHT, KJS, and EJO aided in data collection. GO aided in patent and intellectual property management. YQ, HWT, RCS, and AZ aided in data collection and troubleshooting. JAC and SSK formulated the initial concept, designed experiments, supervised the study, and wrote the manuscript. All authors edited and approved the final version of the manuscript.

REFERENCES:

1. Kitahara CM, Sosa JA. Understanding the ever-changing incidence of thyroid cancer. Nat Rev Endocrinol **2020**;16(11):617-8 doi 10.1038/s41574-020-00414-9.
2. Kim J, Gosnell JE, Roman SA. Geographic influences in the global rise of thyroid cancer. Nat Rev Endocrinol **2020**;16(1):17-29 doi 10.1038/s41574-019-0263-x.
3. Lim H, Devesa SS, Sosa JA, Check D, Kitahara CM. Trends in Thyroid Cancer Incidence and Mortality in the United States, 1974-2013. JAMA **2017**;317(13):1338-48 doi 10.1001/jama.2017.2719.
4. Smallridge RC, Copland JA. Anaplastic thyroid carcinoma: pathogenesis and emerging therapies. Clin Oncol (R Coll Radiol) **2010**;22(6):486-97 doi 10.1016/j.clon.2010.03.013.
5. Jung CK, Bychkov A, Kakudo K. Update from the 2022 World Health Organization Classification of Thyroid Tumors: A Standardized Diagnostic Approach. Endocrinol Metab (Seoul) **2022**;37(5):703-18 doi 10.3803/EnM.2022.1553.
6. Ahmadi S, Stang M, Jiang XS, Sosa JA. Hurthle cell carcinoma: current perspectives. Onco Targets Ther **2016**;9:6873-84 doi 10.2147/OTT.S119980.
7. McFadden DG, Sadow PM. Genetics, Diagnosis, and Management of Hurthle Cell Thyroid Neoplasms. Front Endocrinol (Lausanne) **2021**;12:696386 doi 10.3389/fendo.2021.696386.
8. Viola D, Valerio L, Molinaro E, Agate L, Bottici V, Biagini A*, et al.* Treatment of advanced thyroid cancer with targeted therapies: ten years of experience. Endocr Relat Cancer **2016**;23(4):R185-205 doi 10.1530/ERC-15-0555.
9. French JD. Immunotherapy for advanced thyroid cancers - rationale, current advances and future strategies. Nat Rev Endocrinol **2020**;16(11):629-41 doi 10.1038/s41574-020-0398-9.
10. Maniakas A, Dadu R, Busaidy NL, Wang JR, Ferrarotto R, Lu C*, et al.* Evaluation of Overall Survival in Patients With Anaplastic Thyroid Carcinoma, 2000-2019. JAMA Oncol **2020**;6(9):1397-404 doi 10.1001/jamaoncol.2020.3362.
11. June CH, Sadelain M. Chimeric Antigen Receptor Therapy. **2018**;379:64-73 doi 10.1056/NEJMra1706169.
12. Schuster SJ, Bishop MR, Tam CS, Waller EK, Borchmann P, McGuirk JP*, et al.* Tisagenlecleucel in Adult Relapsed or Refractory Diffuse Large B-Cell Lymphoma. **2018**;380:45-56 doi 10.1056/NEJMoa1804980.
13. Neelapu SS, Locke FL, Bartlett NL, Lekakis LJ, Miklos DB, Jacobson CA*, et al.* Axicabtagene Ciloleucel CAR T-Cell Therapy in Refractory Large B-Cell Lymphoma. N Engl J Med **2017**;377(26):2531-44 doi 10.1056/NEJMoa1707447.
14. Munshi NC, Anderson LD, Jr., Shah N, Madduri D, Berdeja J, Lonial S*, et al.* Idecabtagene Vicleucel in Relapsed and Refractory Multiple Myeloma. N Engl J Med **2021**;384(8):705-16 doi 10.1056/NEJMoa2024850.
15. Maude SL, Laetsch TW, Buechner J, Rives S, Boyer M, Bittencourt H*, et al.* Tisagenlecleucel in Children and Young Adults with B-Cell Lymphoblastic Leukemia. N Engl J Med **2018**;378(5):439-48 doi 10.1056/NEJMoa1709866.
16. Beatty GL, Moon EK. Chimeric antigen receptor T cells are vulnerable to immunosuppressive mechanisms present within the tumor microenvironment. Oncoimmunology **2014**;3(11):e970027 doi 10.4161/21624011.2014.970027.
17. Castellarin M, Watanabe K, June CH, Kloss CC, Posey AD. Driving cars to the clinic for solid tumors. Gene Therapy **2018**;25(3):165-75 doi 10.1038/s41434-018-0007-x.
18. Ma S, Li X, Wang X, Cheng L, Li Z, Zhang C*, et al.* Current Progress in CAR-T Cell Therapy for Solid Tumors. Int J Biol Sci **2019**;15(12):2548-60 doi 10.7150/ijbs.34213.
19. Moghimi B, Barrett D. CAR T Cells for Solid Tumors. Current Stem Cell Reports **2017**;3(4):269-78 doi 10.1007/s40778-017-0101-9.
20. Sterner RC, Sterner RM. CAR-T cell therapy: current limitations and potential strategies. **2021**;11:69 doi 10.1038/s41408-021-00459-7.
21. Kankeu Fonkoua LA, Sirpilla O, Sakemura R, Siegler EL, Kenderian SS. CAR T cell therapy and the tumor microenvironment: Current challenges and opportunities. Mol Ther Oncolytics **2022**;25:69-77 doi 10.1016/j.omto.2022.03.009.
22. Can I, Cox MJ, Siegler EL, Sakemura R, Kenderian SS. Challenges of chimeric antigen receptor T-cell therapy in chronic lymphocytic leukemia: lessons learned. Exp Hematol **2022**;108:1-7 doi

10.1016/j.exphem.2022.02.001.
23. Sakemura R, Cox MJ, Hansen MJ, Hefazi M, Manriquez Roman C, Schick KJ*, et al.* Targeting Cancer Associated Fibroblasts in the Bone Marrow Prevents Resistance to Chimeric Antigen Receptor T Cell Therapy in Multiple Myeloma. Blood **2019**;134(Supplement_1):865- doi 10.1182/blood-2019-123277.
24. Tuncel M. Thyroid Stimulating Hormone Receptor. Mol Imaging Radionucl Ther **2017**;26(Suppl 1):87-91 doi 10.4274/2017.26.suppl.10.
25. Rowe CW, Paul JW, Gedye C, Tolosa JM, Bendinelli C, McGrath S*, et al.* Targeting the TSH receptor in thyroid cancer. Endocr Relat Cancer **2017**;24(6):R191-R202 doi 10.1530/ERC-17-0010.
26. Carayon P, Thomas-Morvan C, Castanas E, Tubiana M. Human thyroid cancer: membrane thyrotropin binding and adenylate cyclase activity. J Clin Endocrinol Metab **1980**;51(4):915-20 doi 10.1210/jcem-51-4-915.
27. Davies TF, Latif R. Targeting the thyroid-stimulating hormone receptor with small molecule ligands and antibodies. Expert Opin Ther Targets **2015**;19(6):835-47 doi 10.1517/14728222.2015.1018181.
28. ElMokh O, Taelman V, Radojewski P, Roelli MA, Stoss A, Dumont RA*, et al.* MEK Inhibition Induces Therapeutic Iodine Uptake in a Murine Model of Anaplastic Thyroid Cancer. J Nucl Med **2019**;60(7):917-23 doi 10.2967/jnumed.118.216721.
29. Liu D, Hu S, Hou P, Jiang D, Condouris S, Xing M. Suppression of BRAF/MEK/MAP kinase pathway restores expression of iodide-metabolizing genes in thyroid cells expressing the V600E BRAF mutant. Clin Cancer Res **2007**;13(4):1341-9 doi 10.1158/1078-0432.CCR-06-1753.
30. Ho AL, Grewal RK, Leboeuf R, Sherman EJ, Pfister DG, Deandreis D*, et al.* Selumetinib-enhanced radioiodine uptake in advanced thyroid cancer. N Engl J Med **2013**;368(7):623-32 doi 10.1056/NEJMoa1209288.
31. Hayes DN, Lucas AS, Tanvetyanon T, Krzyzanowska MK, Chung CH, Murphy BA*, et al.* Phase II efficacy and pharmacogenomic study of Selumetinib (AZD6244; ARRY-142886) in iodine-131 refractory papillary thyroid carcinoma with or without follicular elements. Clin Cancer Res **2012**;18(7):2056-65 doi 10.1158/1078-0432.CCR-11-0563.
32. Landa I, Pozdeyev N, Korch C, Marlow LA, Smallridge RC, Copland JA*, et al.* Comprehensive Genetic Characterization of Human Thyroid Cancer Cell Lines: A Validated Panel for Preclinical Studies. Clin Cancer Res **2019**;25(10):3141-51 doi 10.1158/1078-0432.CCR-18-2953.
33. Ricarte-Filho JC, Ryder M, Chitale DA, Rivera M, Heguy A, Ladanyi M*, et al.* Mutational profile of advanced primary and metastatic radioactive iodine-refractory thyroid cancers reveals distinct pathogenetic roles for BRAF, PIK3CA, and AKT1. Cancer Res **2009**;69(11):4885-93 doi 10.1158/0008-5472.CAN-09-0727.
34. Knauf JA, Fagin JA. Role of MAPK pathway oncoproteins in thyroid cancer pathogenesis and as drug targets. Curr Opin Cell Biol **2009**;21(2):296-303 doi 10.1016/j.ceb.2009.01.013.
35. Uhlen M, Fagerberg L, Hallstrom BM, Lindskog C, Oksvold P, Mardinoglu A*, et al.* Proteomics. Tissue-based map of the human proteome. Science **2015**;347(6220):1260419 doi 10.1126/science.1260419.
36. Gimblet GR, Whitt J, Houson HA, Lin D, Guenter R, Rao TC*, et al.* Thyroid-stimulating hormone receptor (TSHR) as a target for imaging differentiated thyroid cancer. Surgery **2024**;175(1):199-206 doi 10.1016/j.surg.2023.05.045.
37. Liu T, Men Q, Su X, Chen W, Zou L, Li Q*, et al.* Downregulated expression of TSHR is associated with distant metastasis in thyroid cancer. Oncol Lett **2017**;14(6):7506-12 doi 10.3892/ol.2017.7122.
38. D'Agostino M, Sponziello M, Puppin C, Celano M, Maggisano V, Baldan F*, et al.* Different expression of TSH receptor and NIS genes in thyroid cancer: role of epigenetics. J Mol Endocrinol **2014**;52(2):121-31 doi 10.1530/JME-13-0160.
39. Fagin JA, Wells SA, Jr. Biologic and Clinical Perspectives on Thyroid Cancer. N Engl J Med **2016**;375(23):2307 doi 10.1056/NEJMc1613118.
40. Jin N, Jiang T, Rosen DM, Nelkin BD, Ball DW. Dual inhibition of mitogen-activated protein kinase kinase and mammalian target of rapamycin in differentiated and anaplastic thyroid cancer. J Clin Endocrinol Metab **2009**;94(10):4107-12 doi 10.1210/jc.2009-0662.
41. Chakravarty D, Santos E, Ryder M, Knauf JA, Liao XH, West BL*, et al.* Small-molecule MAPK inhibitors restore radioiodine incorporation in mouse thyroid cancers with conditional BRAF activation. J Clin Invest **2011**;121(12):4700-11 doi 10.1172/JCI46382.
42. Subbiah V, Kreitman RJ, Wainberg ZA, Cho JY, Schellens JHM, Soria JC*, et al.* Dabrafenib and Trametinib Treatment in Patients With Locally Advanced or Metastatic BRAF V600-Mutant Anaplastic Thyroid Cancer. J Clin Oncol **2018**;36(1):7-13 doi 10.1200/JCO.2017.73.6785.

43. Min IM, Shevlin E, Vedvyas Y, Zaman M, Wyrwas B, Scognamiglio T*, et al.* CAR T Therapy Targeting ICAM-1 Eliminates Advanced Human Thyroid Tumors. Clin Cancer Res **2017**;23(24):7569-83 doi 10.1158/1078-0432.CCR-17-2008.
44. Bhoj VG, Li L, Parvathaneni K, Zhang Z, Kacir S, Arhontoulis D*, et al.* Adoptive T cell immunotherapy for medullary thyroid carcinoma targeting GDNF family receptor alpha 4. Mol Ther Oncolytics **2021**;20:387-98 doi 10.1016/j.omto.2021.01.012.
45. Li H, Zhou X, Wang G, Hua D, Li S, Xu T*, et al.* CAR-T Cells Targeting TSHR Demonstrate Safety and Potent Preclinical Activity Against Differentiated Thyroid Cancer. J Clin Endocrinol Metab **2022**;107(4):1110-26 doi 10.1210/clinem/dgab819.
46. Xiao L, Liu XC, Zhou KS, Liu Y, Huang Y, Pu CF*, et al.* CoupledCAR technology for treating thyroid cancer. Journal of Clinical Oncology **2021**;39(15) doi 10.1200/JCO.2021.39.15_suppl.e14507.
47. Ding J, Li D, Liu X, Hei H, Sun B, Zhou D*, et al.* Chimeric antigen receptor T-cell therapy for relapsed and refractory thyroid cancer. Exp Hematol Oncol **2022**;11(1):59 doi 10.1186/s40164-022-00311-z.
48. Marlow LA, Rohl SD, Miller JL, Knauf JA, Fagin JA, Ryder M*, et al.* Methodology, Criteria, and Characterization of Patient-Matched Thyroid Cell Lines and Patient-Derived Tumor Xenografts. J Clin Endocrinol Metab **2018**;103(9):3169-82 doi 10.1210/jc.2017-01845.
49. Zielke A, Tezelman S, Jossart GH, Wong M, Siperstein AE, Duh QY*, et al.* Establishment of a highly differentiated thyroid cancer cell line of Hurthle cell origin. Thyroid **1998**;8(6):475-83 doi 10.1089/thy.1998.8.475.
50. Sterner RM, Sakemura R, Cox MJ, Yang N, Khadka RH, Forsman CL*, et al.* GM-CSF inhibition reduces cytokine release syndrome and neuroinflammation but enhances CAR-T cell function in xenografts. Blood **2019**;133(7):697-709 doi 10.1182/blood-2018-10-881722.
51. Dietz AB, Bulur PA, Emery RL, Winters JL, Epps DE, Zubair AC*, et al.* A novel source of viable peripheral blood mononuclear cells from leukoreduction system chambers. Transfusion **2006**;46(12):2083-9 doi 10.1111/j.1537-2995.2006.01033.x.
52. Sanders J, Miguel RN, Furmaniak J, Smith BR. TSH receptor monoclonal antibodies with agonist, antagonist, and inverse agonist activities. Methods Enzymol **2010**;485:393-420 doi 10.1016/B978-0-12-381296-4.00022-1.
53. Cox MJ, Lucien F, Sakemura R, Boysen JC, Kim Y, Horvei P*, et al.* Leukemic extracellular vesicles induce chimeric antigen receptor T cell dysfunction in chronic lymphocytic leukemia. Mol Ther **2021**;29(4):1529-40 doi 10.1016/j.ymthe.2020.12.033.
54. Cox MJ, Manriquez Roman C, Tapper EE, Siegler EL, Chappell D, Durrant C*, et al.* GM-CSF disruption in CART cells modulates T cell activation and enhances CART cell anti-tumor activity. Leukemia **2022** doi 10.1038/s41375-022-01572-7.
55. Sakemura R, Bansal A, Siegler EL, Hefazi M, Yang N, Khadka RH*, et al.* Development of a Clinically Relevant Reporter for Chimeric Antigen Receptor T-cell Expansion, Trafficking, and Toxicity. Cancer Immunol Res **2021**;9(9):1035-46 doi 10.1158/2326-6066.CIR-20-0901.
56. Sakemura RL, Hefazi M, Cox MJ, Siegler EL, Sinha S, Hansen MJ*, et al.* AXL Inhibition Improves the Antitumor Activity of Chimeric Antigen Receptor T Cells. Cancer Immunol Res **2023**;11(9):1222-36 doi 10.1158/2326-6066.CIR-22-0254.
57. Sakemura R, Hefazi M, Siegler EL, Cox MJ, Larson DP, Hansen MJ*, et al.* Targeting Cancer-Associated Fibroblasts in the Bone Marrow Prevents Resistance to CART-Cell Therapy in Multiple Myeloma. Blood **2022** doi 10.1182/blood.2021012811.

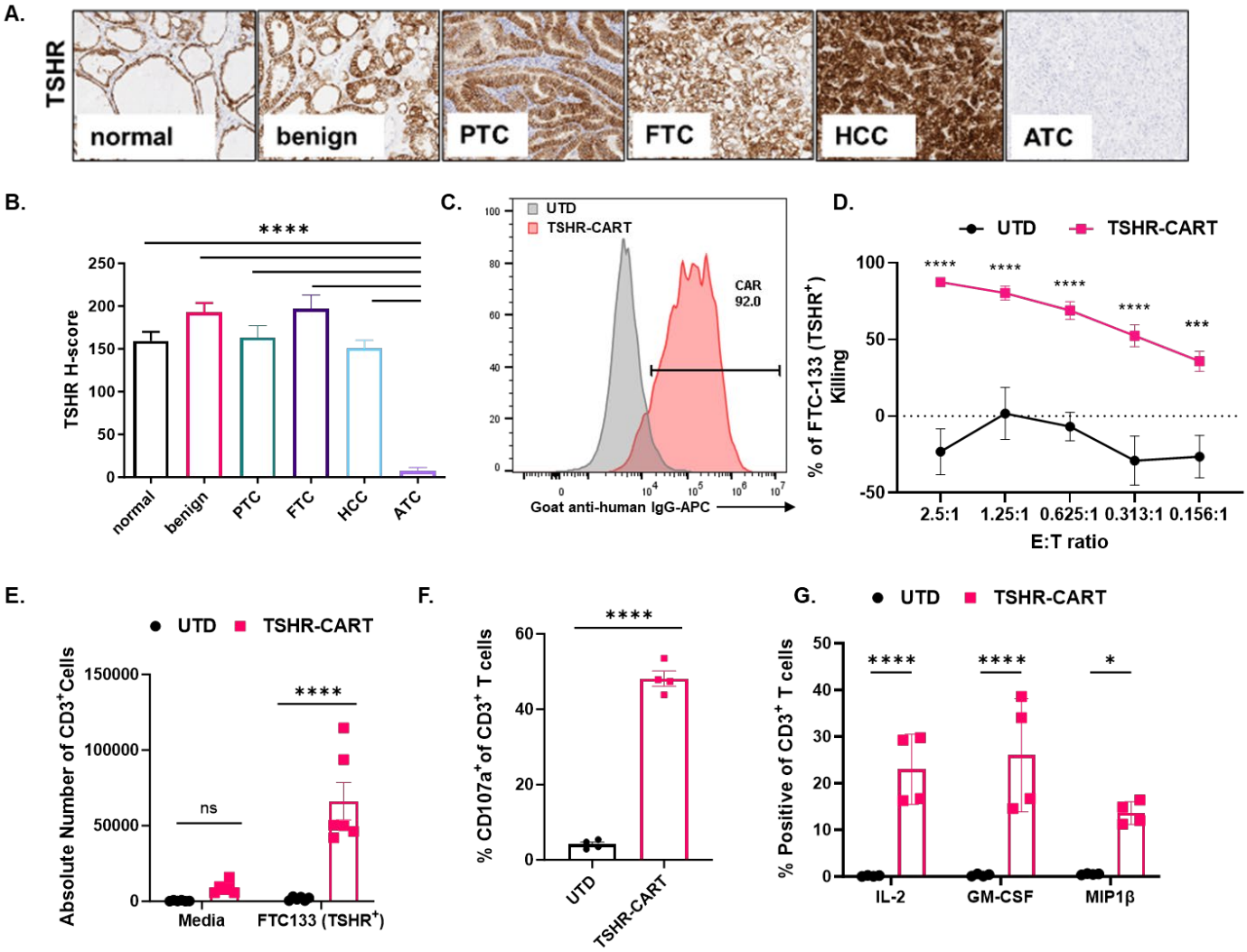

Figure 1. TSHR is a rational target for CART cell therapy, and TSHR-CART cells demonstrate antigen-specific effector functions in vitro. A) Representative IHC staining shows TSHR expression across normal, benign, and malignant thyroid tissues. IHC demonstrated robust TSHR expression in all sampled thyroid tissue subtypes except for ATC. PTC: papillary thyroid cancer; FTC: follicular thyroid cancer; HCC: Hurthle cell carcinoma; ATC: anaplastic thyroid cancer. **B)** H-score quantitation of TSHR expression is shown. H-scores of ATC samples were significantly lower than other thyroid tissues. H-scores provided are based on 0 – 3 IHC scoring and percentage of total areas each score (0x%0 + 1x%1 + 2x%2 + 3x%3 = H Score; 0 – 300 range with statistical analysis. ****p < 0.0001, one-way ANOVA; normal n = 11, benign n = 9, PTC n = 11, FTC n = 9, HCC n = 37, ATC n = 10). **C)** Representative histogram shows CAR expression on TSHR-CART cells as determined by flow cytometry. TSHR-targeting CARs were strongly expressed on human T cells from healthy donors. UTD T cells were used as a negative control. **D)** Luciferase$^+$ TSHR$^+$ FTC133 target cells were co-cultured with either UTD or TSHR-CART cells at varying effector-to-target ratios, and cytotoxicity was measured via bioluminescence after 24 hours. TSHR-CART cells exhibited potent antigen-specific killing against the target cells (mean and SEM; ***p< 0.001, ****p < 0.0001, two-way ANOVA; 3 biological replicates). **E)** UTD or TSHR-CART cells were co-cocultured with either media alone (negative control) or TSHR$^+$ FTC133 target cells. After five days, T cell proliferation was assessed by flow cytometry using absolute counts of CD3$^+$ cells. TSHR-CART cells demonstrated significant antigen-specific proliferation (mean and SEM; ****p < 0.0001, two-way ANOVA; 3 biological replicates). **F)** UTD or TSHR-CART cells were-cocultured with TSHR$^+$ FTC133 target cells at a 1:5 ratio for four hours, and degranulation was then assessed by flow cytometry of CD3$^+$ CD107a$^+$ cells (mean and SEM; ****p < 0.0001, unpaired two-tailed t-test; 2 biological replicates). **G)** UTD or TSHR-CART cells were-cocultured with TSHR$^+$ FTC133 target cells at a 1:5 ratio for four hours, and cytokine production was then assessed by intracellular cytokine staining and flow cytometry of CD3$^+$ cells (mean and SEM; *p < 0.05, ****p < 0.0001, two-way ANOVA; 2 biological replicates).

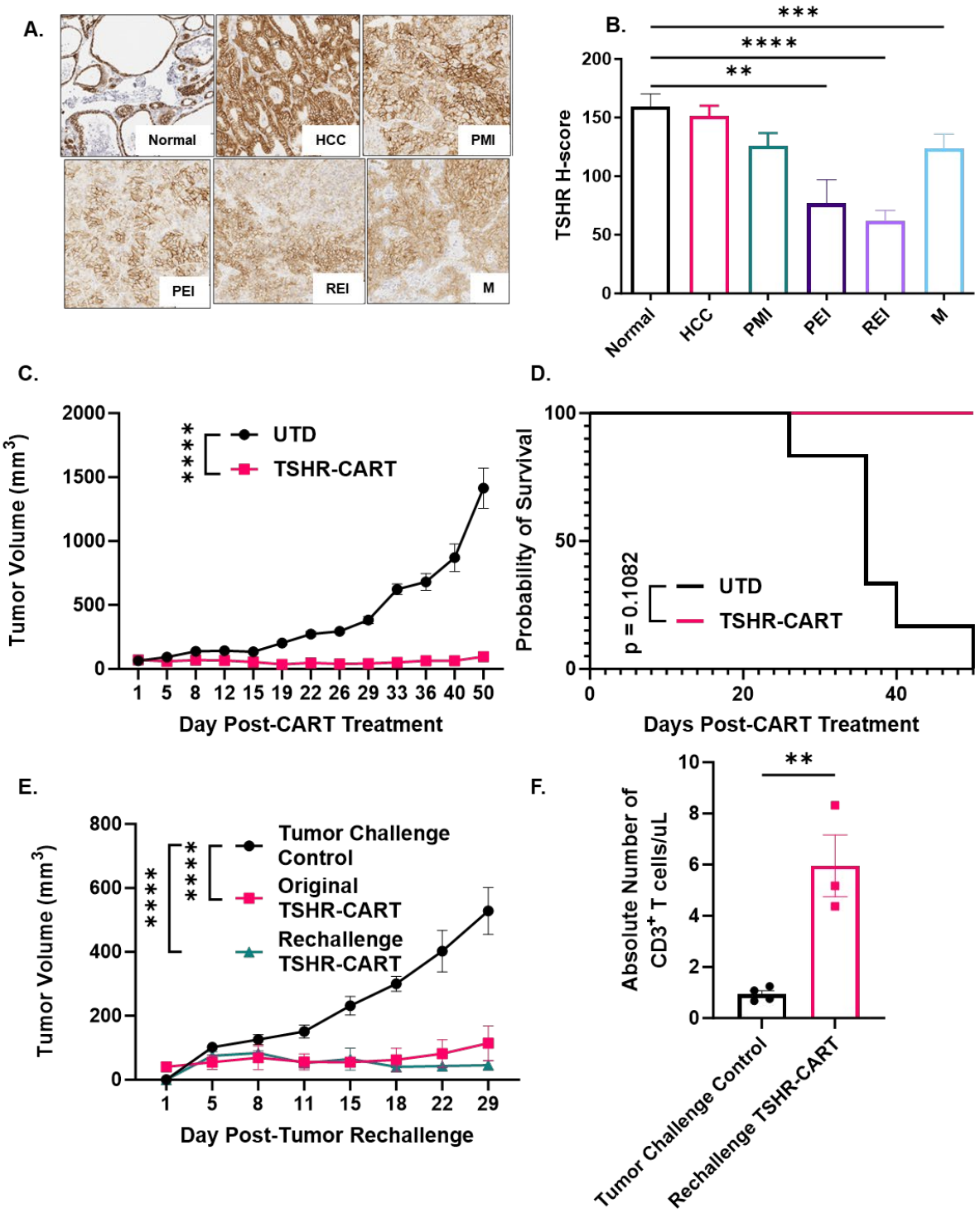

Figure 2. TSHR-CART cells exhibit potent antitumor activity in vivo against Hurthle cell carcinoma. A) Tissue microarray slides with patient samples representing normal thyroid tissue (Normal, n=11), Hurthle cell carcinoma (HCC, n=37), primary tumor with minimal invasion (PMI, n=26), primary tumor with extensive invasion (PEI, n=11), recurrent tumor with extensive invasion (REI, n=34) and metastatic tumors (M, n=16) were stained for TSHR via IHC. **B)** TSHR expression was quantified using H-Score (based on 0 – 300 IHC scoring and percentage of total areas each score, 0 – 300 range with statistical analysis). * $p < 0.05$, *** $p < 0.001$, **** $p < 0.0001$, one-way ANOVA. **C)** Tumor volume was assessed via serial caliper measurements, which revealed significant tumor regression in TSHR-CART-treated mice (mean and SEM; ****$p < 0.0001$, two-way ANOVA; n=6 mice per group). **D)** Kaplan-Meier survival curve demonstrated prolonged survival in mice treated with TSHR-CART compared to UTD ($p = 0.1082$, Log-rank test; n=6 mice per group). **E)** Tumor volume was significantly suppressed in both original and rechallenge tumors in TSHR-CART-treated mice (mean and SEM; ****$p < 0.0001$, two-way ANOVA; n=6 mice per group). **F)** Peripheral blood was collected 21 days after tumor rechallenge, and TSHR-CART-treated mice showed significantly greater T cell proliferation as assessed by flow cytometry using absolute counts of $CD3^+$ cells (mean and SEM; ****$p < 0.0001$, two-tailed unpaired t-test; n = 3 mice per group).

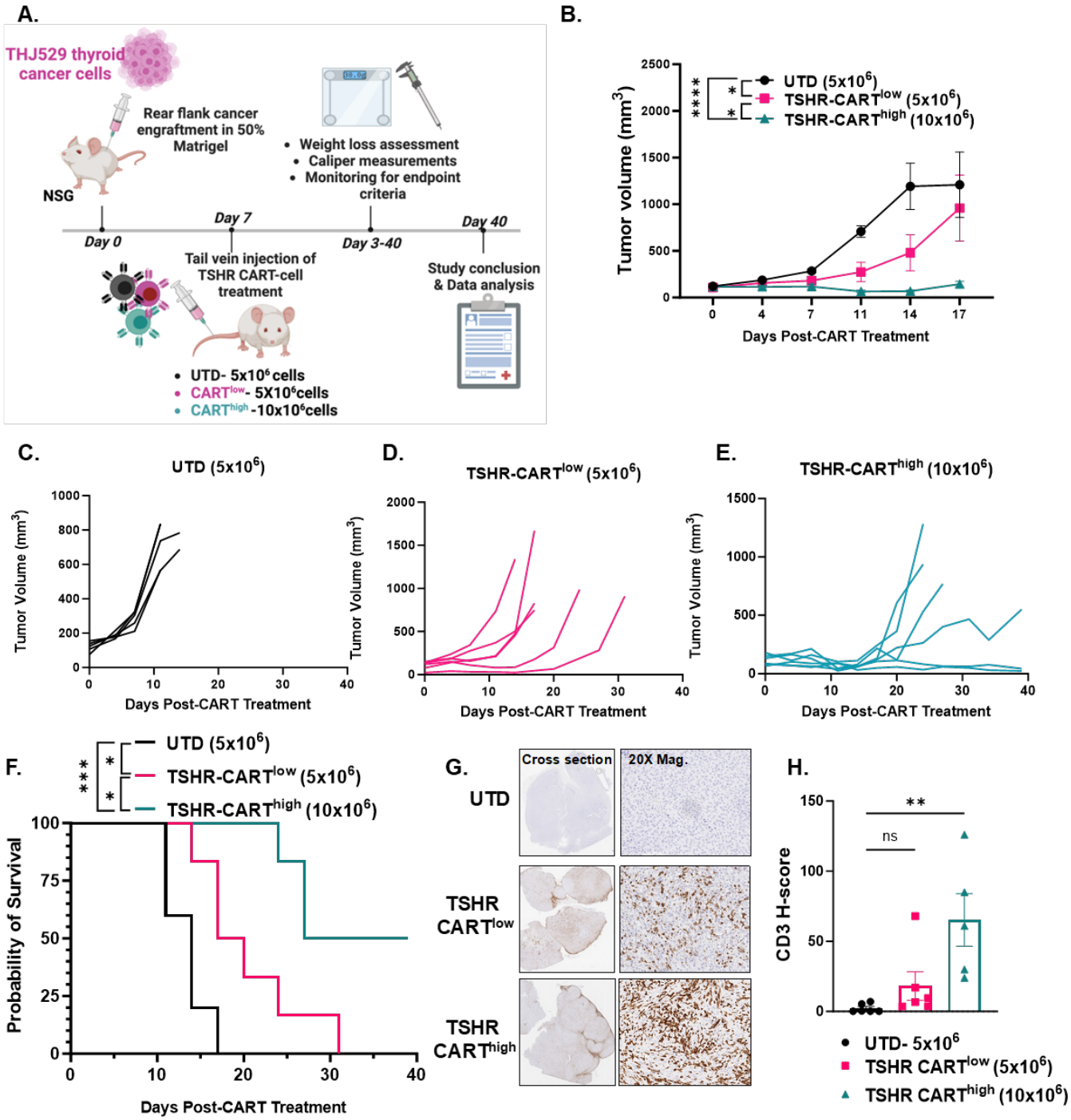

Figure 3. TSHR-CART cells exhibit dose-dependent antitumor activity in vivo. A) Experimental schema of a PDTC xenograft model. NSG mice were subcutaneously engrafted with TSHR$^+$ THJ529 thyroid cancer cells in Matrigel. One week later, after engraftment was confirmed, mice were randomized according to tumor volume and received either UTD (5 x 10^6) or TSHR-CART cells (5 x 10^6 or 1 x 10^7) intravenously. Mice were monitored for well-being, tumor volume, and overall survival. **B)** Tumor volume was assessed via serial caliper measurements, which revealed dose-dependent tumor regression in TSHR-CART-treated mice (mean and SEM; *$p < 0.05$, ****$p < 0.0001$, two-way ANOVA; n=6 mice per group). **C-E)** Individual tumor growth curves are shown for each treatment group. **F)** Kaplan-Meier survival curve demonstrated significantly prolonged survival in mice treated with TSHR-CART compared to UTD (*$p < 0.05$, ***$p < 0.001$, Log-rank test; n=6 mice per group). **G)** Representative IHC staining shows human CD3 expression in thyroid tumors excised from mice in each treatment group. T cell infiltration into the tumor was significantly higher in TSHR-CART^{high}-treated mice. **H)** H-score quantitation of human CD3 expression is shown. H-scores of tumors from mice treated with TSHR-CART^{high} were significantly increased compared to other treatment groups. H-scores provided are based on 0 – 3 IHC scoring and percentage of total areas each score (0x%0 + 1x%1 + 2x%2 + 3x%3 = H Score; 0 – 300 range with statistical analysis. Mean and SEM; **$p < 0.01$, one-way ANOVA; n = 5-6 mice per group).

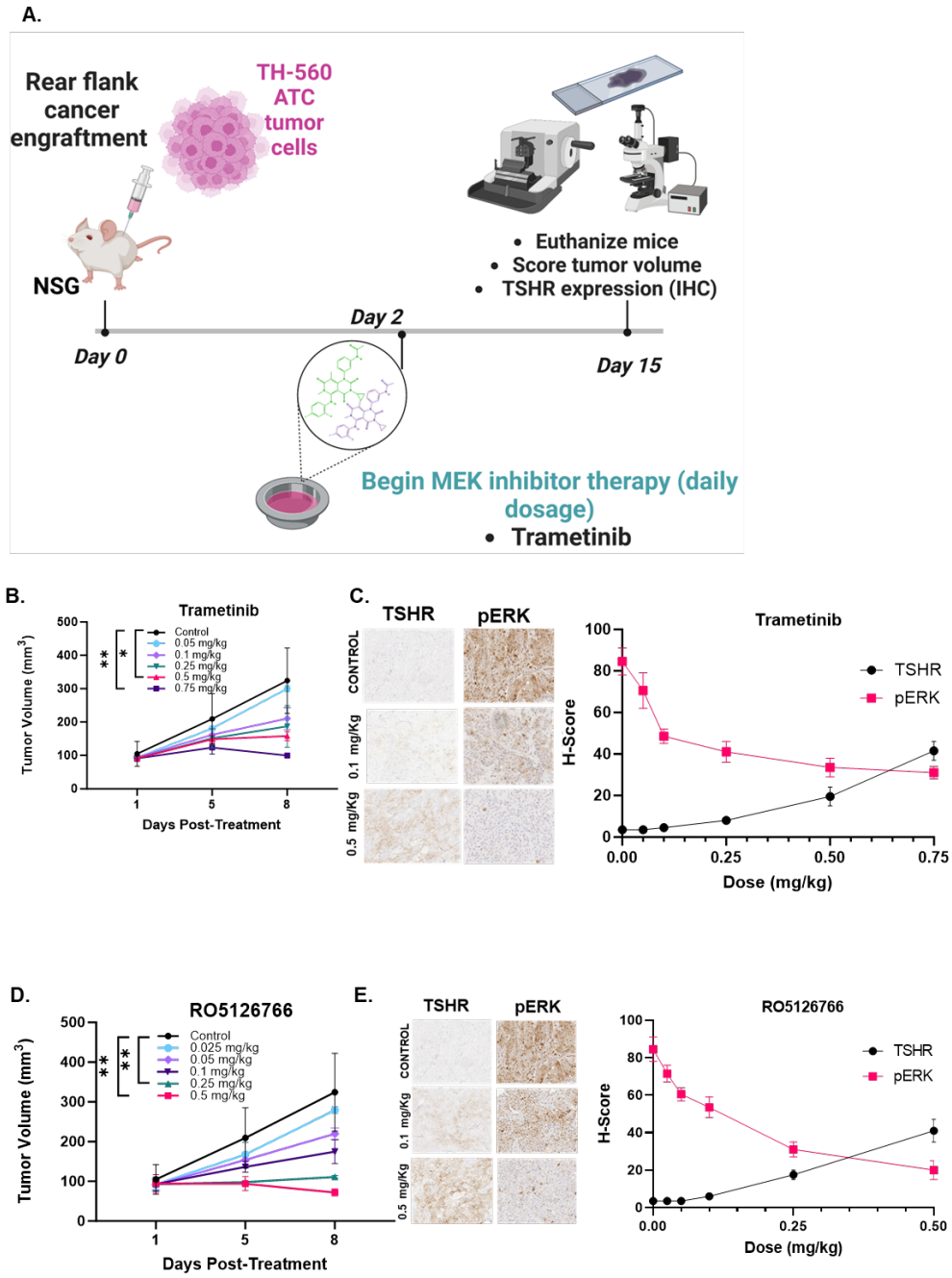

Figure 4. Treatment of ATC PDX tumors with MAPK inhibitors restores TSHR expression. A) Experimental schema of an ATC PDX model. NSG mice were subcutaneously engrafted with Th-560 ATC PDX tumors. When tumors reached approximately 100 mm^3, mice were orally treated with MAPK inhibitors daily and serially monitored for tumor volume. On Day 15, mice were sacrificed, and tumors were harvested and assessed for TSHR expression by IHC. **B)** Tumor volumes were assessed via serial caliper measurements in mice treated with trametinib at the indicated doses. Trametinib treatment resulted in dose-dependent control of tumor growth (mean and SEM; *$p < 0.05$, **$p < 0.01$, two-way ANOVA; n=2 mice per group). **C)** Representative IHC staining (left) shows human TSHR and pERK expression in thyroid tumors excised from mice in each treatment group. H-score quantitation (right) showed a dose-dependent and inversely proportional relationship between TSHR and pERK expression. H-scores provided are based on 0 – 3 IHC scoring and percentage of total areas each score (0x%0 + 1x%1 + 2x%2 + 3x%3 = H Score; 0 – 300 range with statistical analysis. Mean and SEM; n = 2 mice per group). **D)** Tumor volumes were assessed via serial caliper measurements in mice treated with RO5126766 at the indicated doses. RO5126766 treatment resulted in dose-dependent control of tumor growth (mean and SEM; *$p < 0.05$, **$p < 0.01$, two-way ANOVA; n=2 mice per group). **E)** Representative IHC staining (left) shows human TSHR and pERK expression in thyroid tumors excised from mice in each treatment group. H-score quantitation (right) showed a dose-dependent and inversely proportional relationship between TSHR and pERK expression. H-scores provided are based on 0 – 3 IHC scoring and percentage of total areas each score (0x%0 + 1x%1 + 2x%2 + 3x%3 = H Score; 0 – 300 range with statistical analysis. Mean and SEM; n = 2 mice per group).

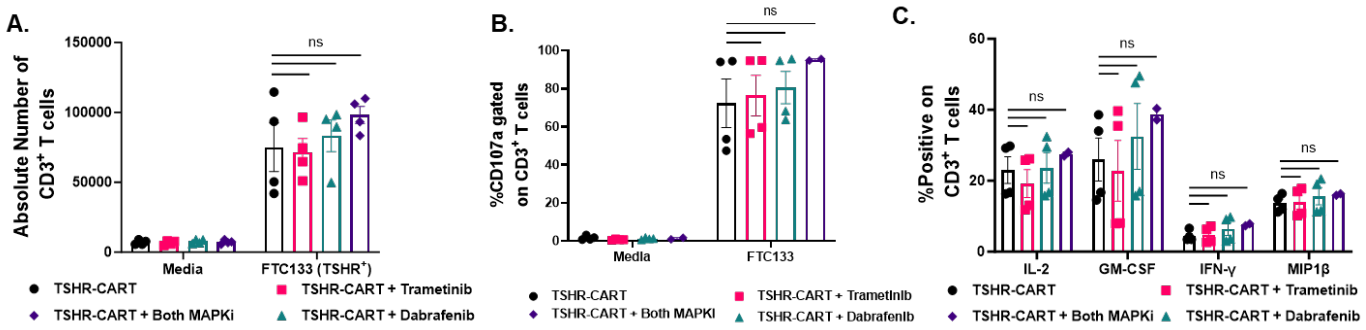

Figure 5. CART effector functions remain intact after the addition of MAPK inhibitors. A) UTD or TSHR-CART cells were co-cocultured with either media alone (negative control) or TSHR$^+$ FTC133 target cells at a 1:1 ratio, along with vehicle control, 10nM trametinib, 10nM dabrafenib, or 10nM both trametinib and dabrafenib. After five days, T cell proliferation was assessed by flow cytometry using absolute counts of CD3$^+$ cells. TSHR-CART cells demonstrated significant antigen-specific proliferation with no statistical differences between MAPK inhibitor-treated groups and control group (mean and SEM; two-way ANOVA; 2 biological replicates). **B)** UTD or TSHR-CART cells were-cocultured with TSHR$^+$ FTC133 target cells at a 1:5 ratio, along with vehicle control, 10nM trametinib, 10nM dabrafenib, or 10nM both trametinib and dabrafenib. After four hours, degranulation was assessed by flow cytometry of CD3$^+$ CD107a$^+$ cells. TSHR-CART cells demonstrated significant antigen-specific degranulation with no statistical differences between MAPK inhibitor-treated groups and control group (mean and SEM; two-way ANOVA; 2 biological replicates). **C)** UTD or TSHR-CART cells were cocultured with TSHR$^+$ FTC133 target cells at a 1:5 ratio, along with vehicle control, 10nM trametinib, 10nM dabrafenib, or 10nM both trametinib and dabrafenib. After four hours, cytokine production was assessed by intracellular cytokine staining and flow cytometry of CD3$^+$ cells. TSHR-CART cells demonstrated significant antigen-specific cytokine production with no statistical differences between MAPK inhibitor-treated groups and control group (mean and SEM; two-way ANOVA; 2 biological replicates).

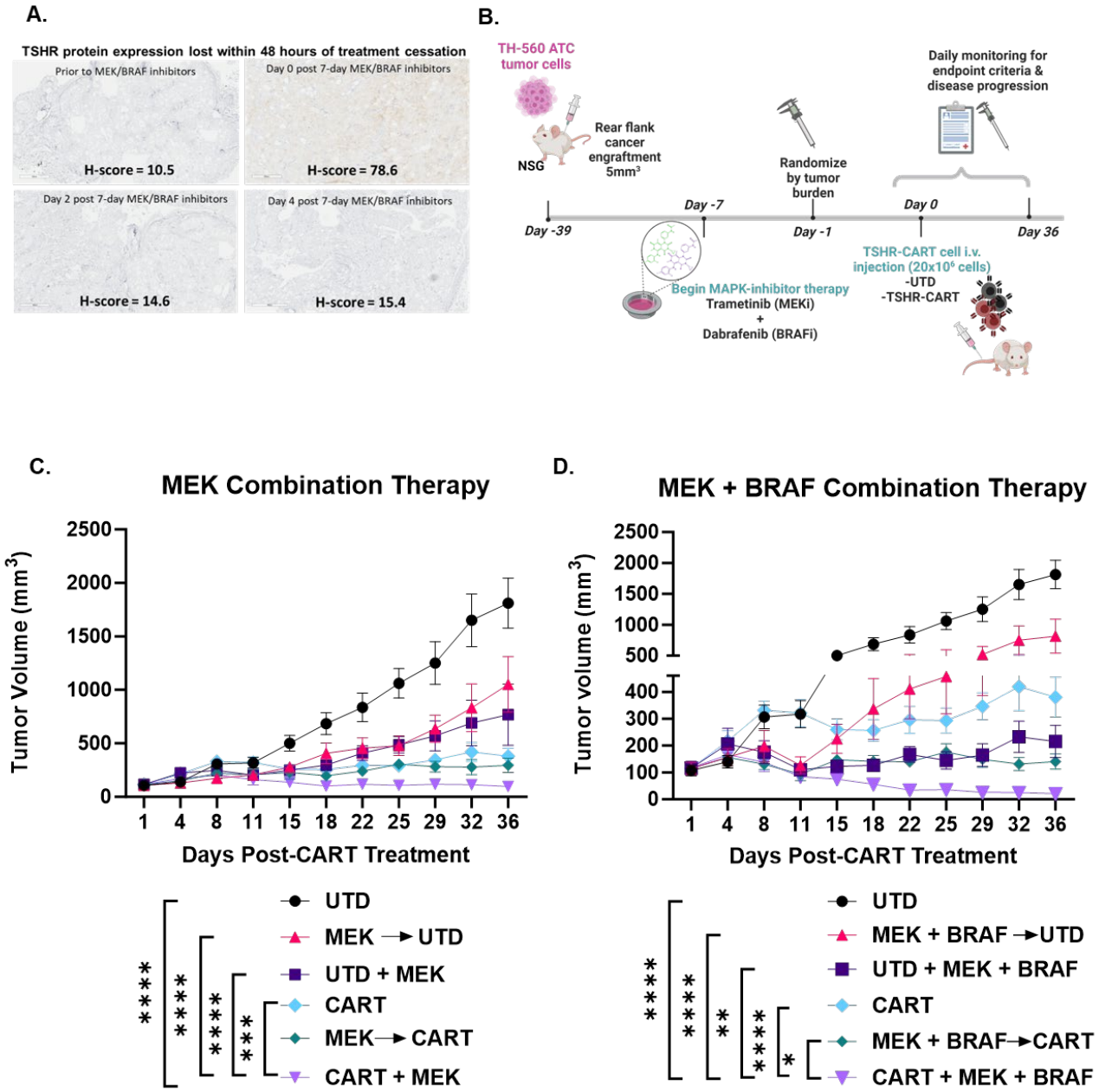

Figure 6. TSHR-CART cells showed the most potent antitumor activity when combined with continuous MAPK inhibitor administration. A) NSG mice were subcutaneously engrafted with TSHR$^+$ THJ529 thyroid cancer cells in Matrigel. One week later, after engraftment was confirmed, mice were treated orally with 1.5 mg/kg dual MEK/BRAF inhibitor R05126766 plus 1 mg/kg dabrafenib daily for 7 days. Representative IHC staining shows human TSHR expression in thyroid tumors excised from mice at various timepoints. TSHR expression was upregulated immediately after 7 days of MAPK inhibitor but was lost within two days after the inhibitors were stopped. H-scores provided are based on 0 – 3 IHC scoring and percentage of total areas each score (0x%0 + 1x%1 + 2x%2 + 3x%3 = H Score; 0 – 300 range with statistical analysis). **B)** Experimental schema of an ATC PDX model. NSG mice were subcutaneously engrafted with Th-560 ATC PDX tumors. When tumors reached approximately 100 mm^3, mice were orally treated with MAPK inhibitors (0.25 mg/kg trametinib alone or with 2 mg/kg dabrafenib) daily for either seven days or continuously (until endpoints were reached) and serially monitored for tumor volume. Mice were then randomized by tumor volume and treated with either UTD or TSHR-CART cells (20x10^6 intravenously). Mice were monitored for well-being and tumor volume. **C)** Tumor volumes were assessed via serial caliper measurements in mice treated with UTD or TSHR-CART alone, with 7 days of trametinib, or with continuous trametinib at the indicated doses. TSHR-CART cells with continuous trametinib treatment resulted in superior control of tumor growth (mean and SEM; ***$p < 0.001$, ****$p < 0.0001$, two-way ANOVA; n=7 mice per group). **D)** Tumor volumes were assessed via serial caliper measurements in mice treated with UTD or TSHR-CART alone, with 7 days of trametinib plus dabrafenib, or with continuous trametinib plus dabrafenib at the indicated doses. TSHR-CART cells with continuous trametinib plus dabrafenib treatment resulted in superior control of tumor growth (mean and SEM; *$p < 0.05$, **$p < 0.01$, ****$p < 0.0001$, two-way ANOVA; n=7 mice per group).